Enzyme-Mediated Depletion of Serum L-Met Abrogates Prostate Cancer Growth via Multiple Mechanisms without Evidence of Systemic Toxicity in Mice

Appendix

Figure S1

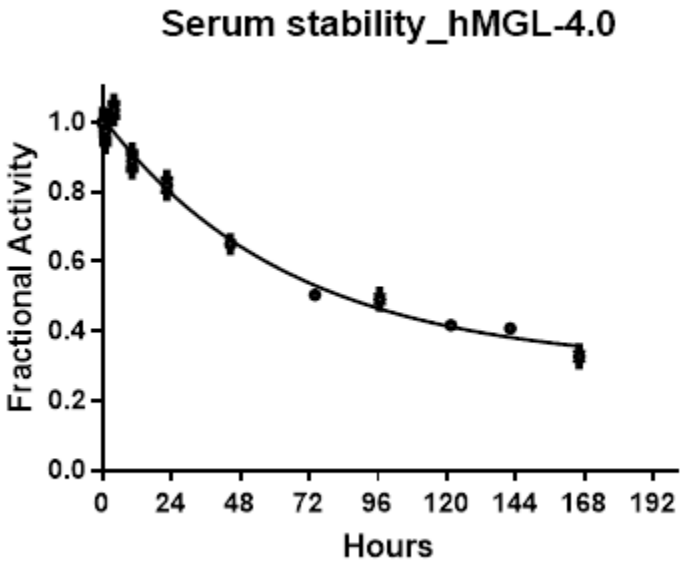

Fig. S1: Assessment of hMGL-4.0 catalytic stability. PEGylated hMGL-4.0 was incubated in pooled human serum at 37 °C and activity was determined as a function of time. An activity half-life was calculated to be 83 ± 2 hrs.

Figure S2

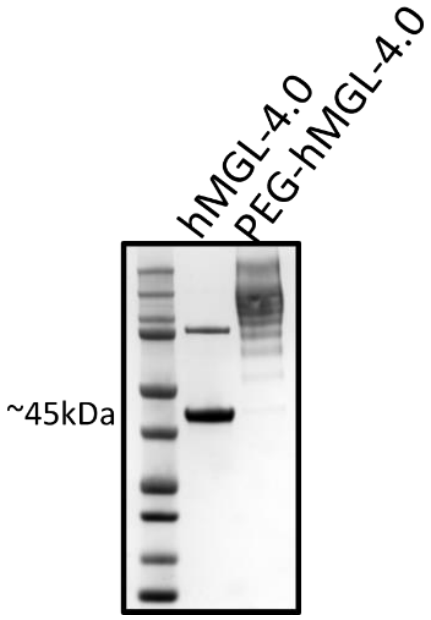

Fig. S2: PEGylation analysis of hMGL-4.0. SDS-PAGE gel of purified hMGL-4.0 (lane 1) and hMGL-4.0 after PEGylation with 100 fold molar excess of methoxy PEG succinimidyl carboxymethyl ester, MW 5000 Da (lane 2).

Table S1

Data Collection	
Wavelength (Å)	1.03321
Resolution range (Å)	50-2.73 (2.78-2.73)[1]
Space Group	P2 2_12_1
Unit cell dimensions	
a, b, c (Å)	113.6, 164.3, 181.7
α, β, Y(˚)	90, 90, 90
Total Reflections	572371
Unique reflections	91209(4400)
Multiplicity	6.3(5.7)
Completeness (%)	99.4(97.6)
Mean I/sigma (I)	13.109(2.260)
R_{merge}	0.129(0.657)

Refinement	
R_{work}	0.1806
R_{free}	0.2290[2]
Number of non-hydrogen atoms	24368
macromolecules	23852
ligands(PLP)	120
solvent	396
Protein residues	3093
RMSD (bonds) (Å)	0.004
RMSD (angles) (˚)	0.677
Ramachandran Favored (%)	96.7
Ramachandran Allowed (%)	3.3
Ramachandran outliers (%)	0.0
Average B-factor (Å^2)	43.1
macromolecules	43.3
ligands(PLP)	44.1
solvent	33.0
MolProbity score	1.59[3](100th percentile[4])

[1]Statistics for the highest resolution shell is shown in parenthesis

[2]R_{free} was calculated by keeping aside 5% of the reflections as an unbiased test set.

[3]The MolProbity score represents a combination of the clashscore, rotamer, and Ramachandran evaluations.

[4]100th percentile represents the best structure of comparable resolution whereas 0th percentile indicates the worst.

Figure S3

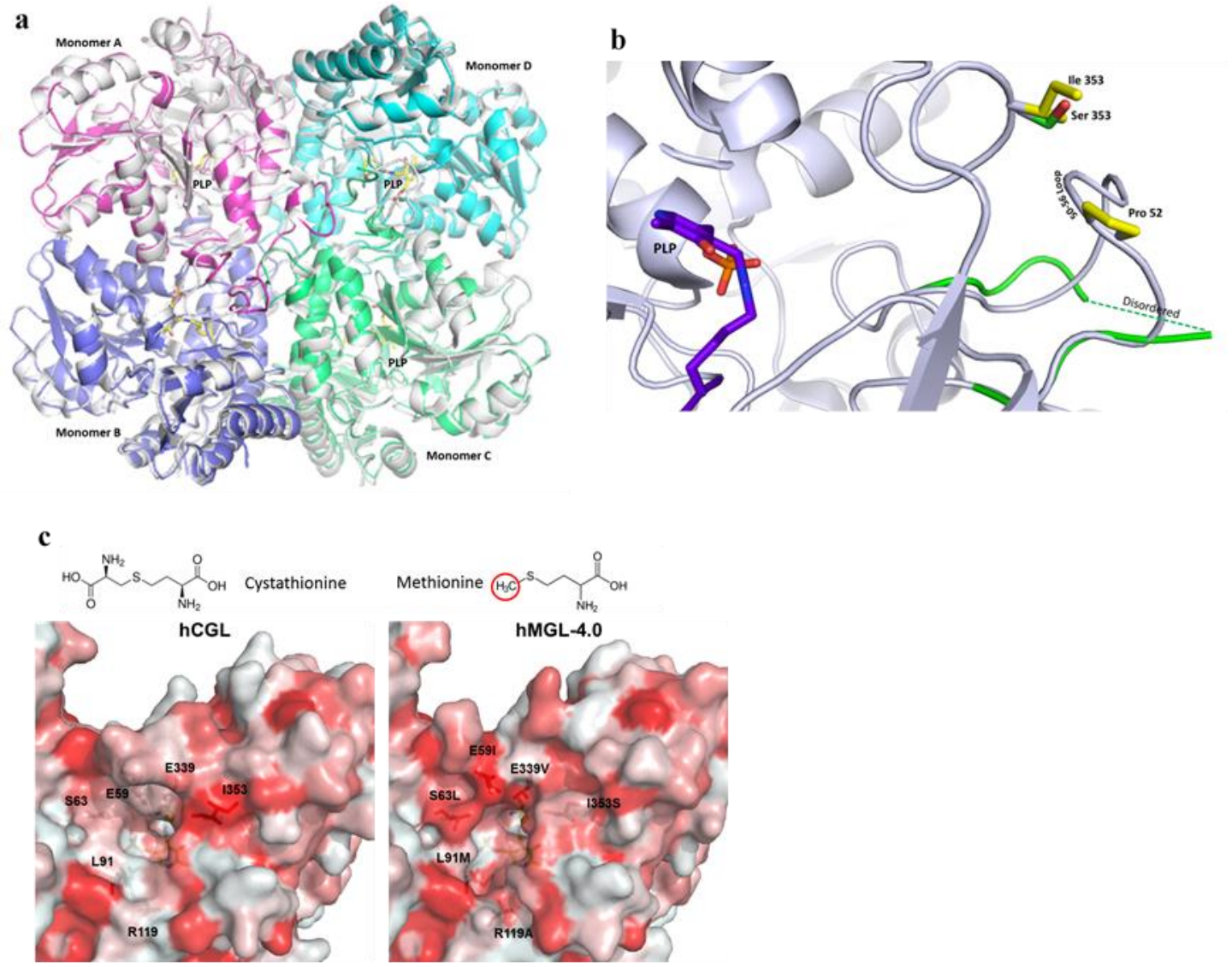

Fig. S3. **Structural analyses of hMGL-4.0.**
(a) Superimposition of the hMGL-4.0 (pdb code: 6OVG) shown in colors with the wild type hCGL shown in white (pdb code: 2NMP). PLP is shown in stick with carbon atoms colored yellow. **(b)** Residues Ile 353 and Pro 52 (shown as yellows sticks) form hydrophobic interactions in the wild-type hCGL. In hMGL-4.0, the I353S mutation (shown in green) destabilizes this interaction leading to a disordering of the 50-56 amino acid loop. The PLP cofactor is shown as sticks with carbon atoms colored purple. **(c)** The comparison of wildtype and hMGL-4.0. A hydrophobicity map of hCGL (PDB: 2NMP) and hMGL-4.0 (pdb code: 6OVG). The E59I, S63L and E339V mutations increase the hydrophobicity of hMGL-4.0 (right) as compared to hCGL facilitating utilization of L-Met as a substrate (Hydrophobic regions indicated in red).

Figure S4

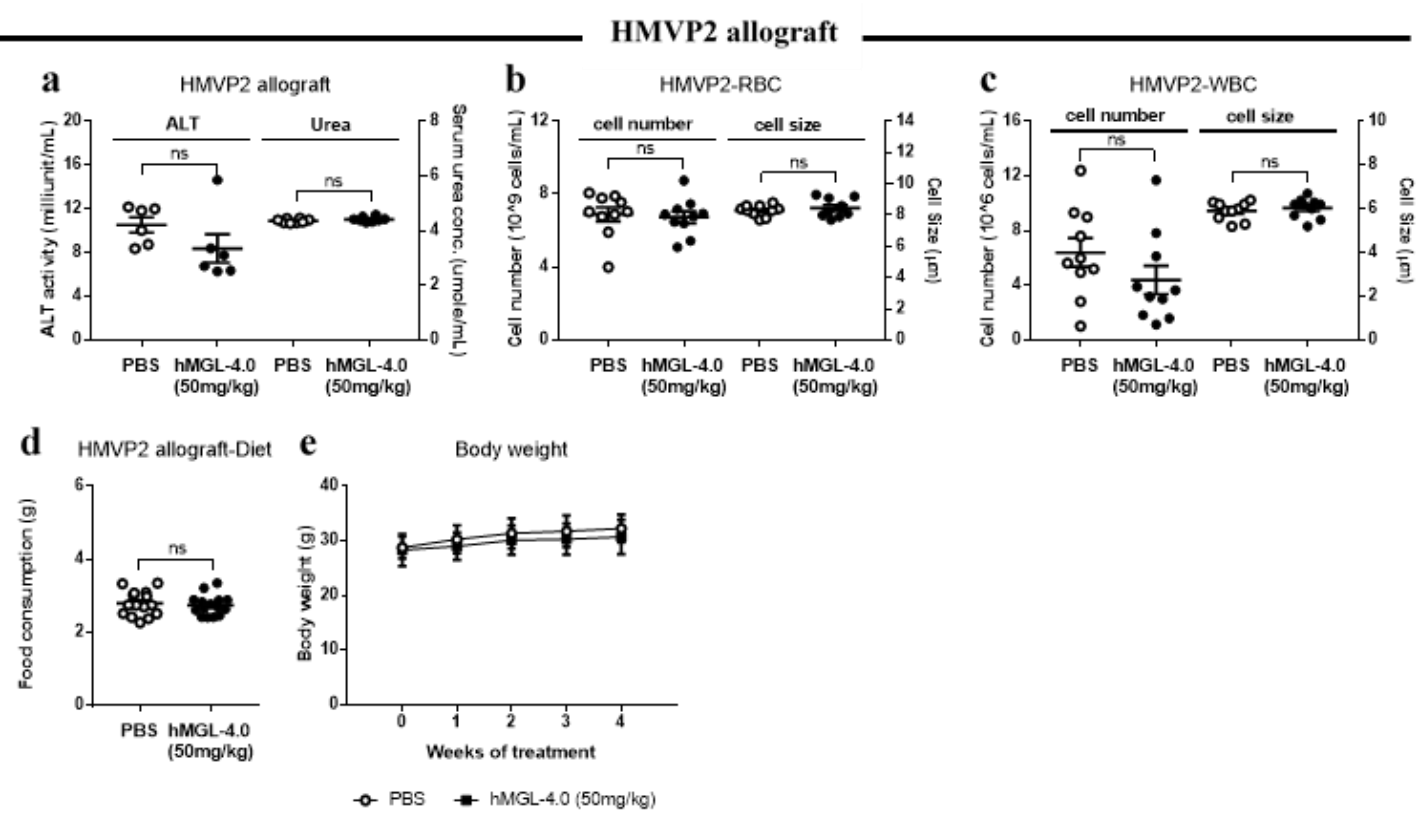

Fig. S4. Toxicological assessment of mice bearing HMVP2 tumors. (a) Renal function was assessed by monitoring serum urea concentrations, and liver toxicity was assessed by serum alanine transaminase (ALT) activity following termination of the HMVP2 allograft studies (ALT group, n = 6 ; urea group, n= 8). **(b, c)** Effect of hMGL-4.0 treatment in FVB/N mice on blood cell count and size, following termination of the HMVP2 allograft studies: **(b)** red blood cell (RBC) number and size; **(c)** white blood cell (WBC) count and and size (n = 10 per group). **(d, e)** Quantitation of average **(d)** food consumption (n=15) per mouse per day and **(e)** body weight (n=10) for each treatment group following treatment with hMGL-4.0 or controls in male FVB/N mice bearing allograft tumors of HMVP2 PCa spheroids. Throughout, data are expressed as mean ± s.e.m. and were found to be not significant; two-tailed Student's t-test.

Figure S5

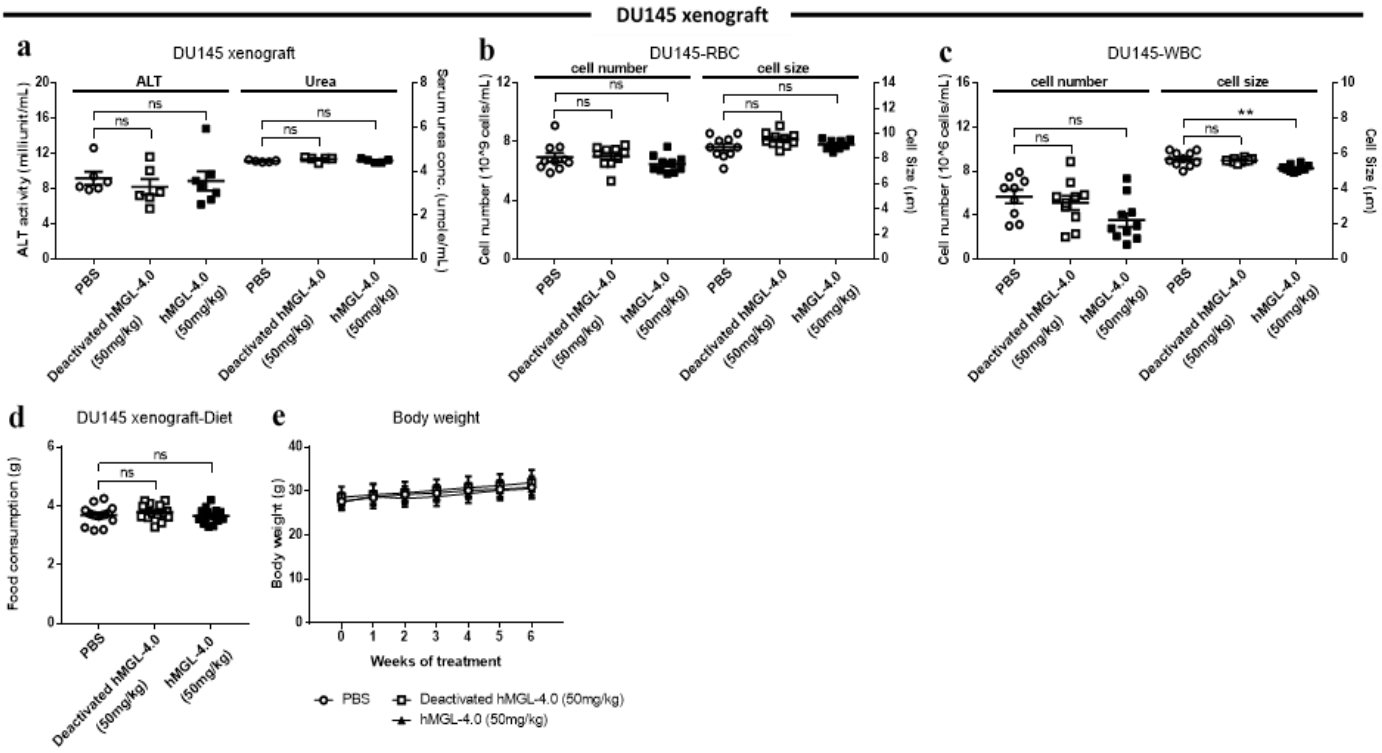

Fig. S5. Toxicological assessment of mice bearing DU145 tumors.
(a) Renal function was assessed by monitoring serum urea concentrations and liver toxicity was assessed by serum alanine transaminase (ALT) activity at sacrifice (ALT group, n = 6 or 8; urea group, n= 5) following treatment with hMGL-4.0 or control, deactivated enzyme in male nude mice bearing DU145 PCa xenografts. **(b, c)** Effect of hMGL-4.0 treatment on blood cell count and size, following termination of the DU145 xenograft studies: **(b)** red blood cell (RBC) number and size; **(c)** white blood cell (WBC) count and and size (n = 10 per group). **(d, e)** Quantitation of average **(d)** food consumption (n=15) per mouse per day and **(e)** body weight (n=10 or 9). Throughout, data are expressed as mean ± s.e.m.; One-way ANOVA (a-d) or two-way ANOVA (e) followed by Bonferroni's multiple comparison test. **P < 0.01.

Figure S6

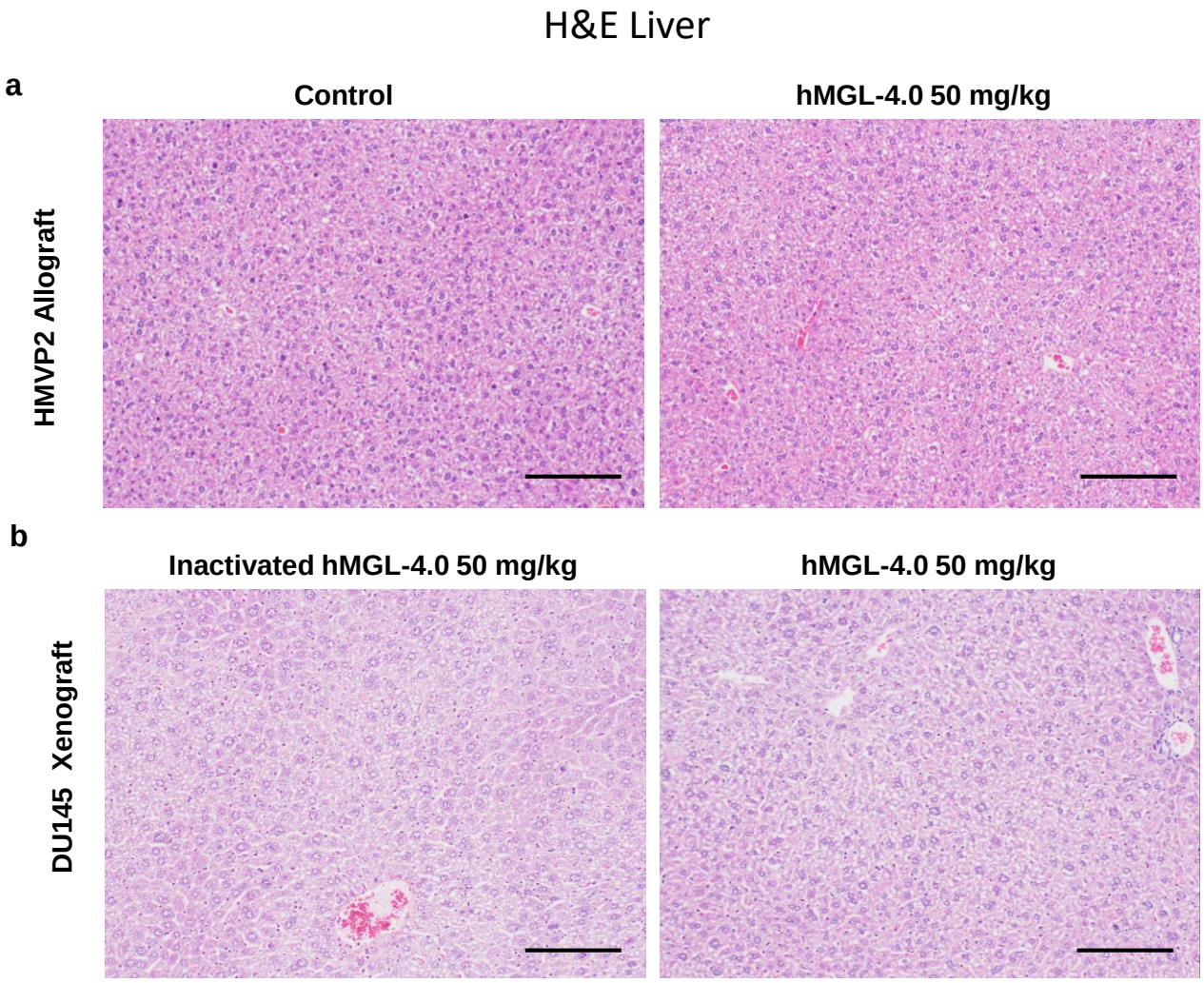

Fig. S6. Histology of liver section of mice bearing HMVP2 and DU145 tumors.
H&E staining of representative liver section of (**a**) FBV/N mice bearing HMVP2 allograft or (**b**) athymic nude mice bearing DU145 xenograft and treated with control (either PBS or heat inactivated hMGL-4.0) or hMGL-4.0 50 mg/kg. Scale bar 100 uM.

Figure S7

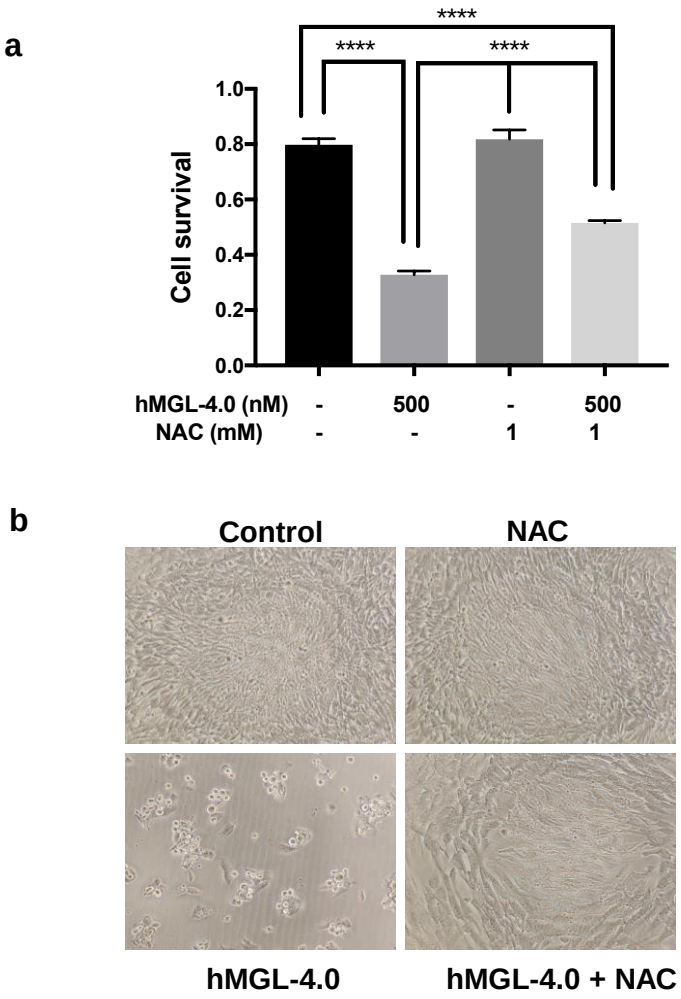

Fig. S7. NAC partially rescues the inhibition of cell survival by hMGL-4.0.
(a) HMVP2 cells were treated with hMGL-4.0, NAC or their combination and cell survival was measured by crystal violet assay. (b) Representative images of cells from (a). Data are expressed as mean ± s.e.m. One-way ANOVA followed by Bonferroni's multiple comparison test. **** $P < 0.0001$.

Figure S8

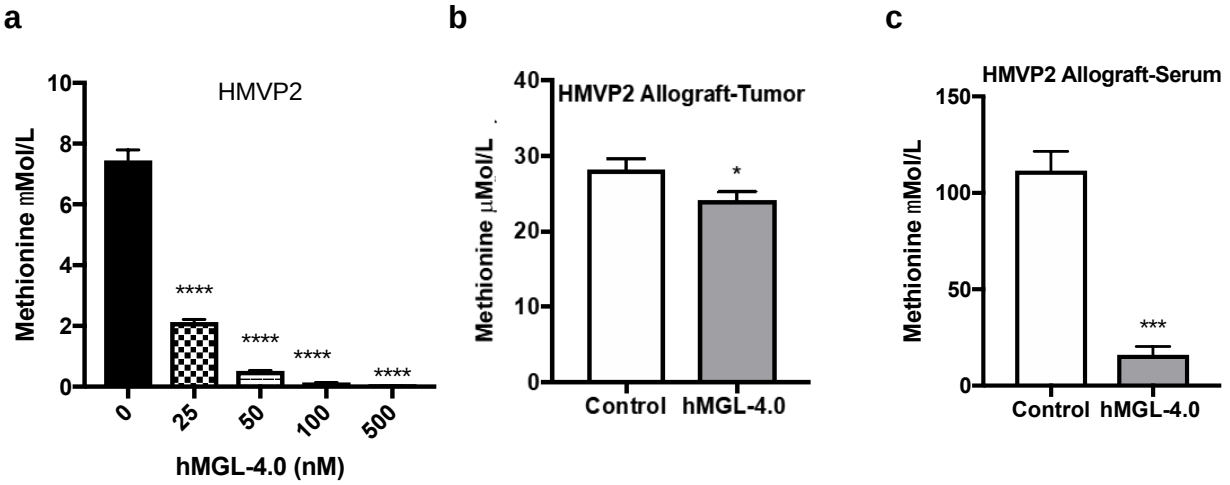

Fig. S8. Absolute L-Met levels. (a) Absolute concentrations of methionine in HMVP2 cells treated *in vitro* with indicated concentrations of hMGL-4.0 (n = 3 cell culture replicates); (b) L-Met levels in HMVP2 tumor tissue (n=8 or 9 for control and hMGL-4.0 50 mg/kg treated tumor tissues) and (c) in serum (n=5) of HMVP2 tumor bearing mice treated with PEG-hMGL-4.0. Data are expressed as mean ± s.e.m. One-way ANOVA followed by Bonferroni's multiple comparison test (a), Student t-test (b, c) . *P < 0.05, ***P < 0.001, **** P < 0.0001.

Figure S9

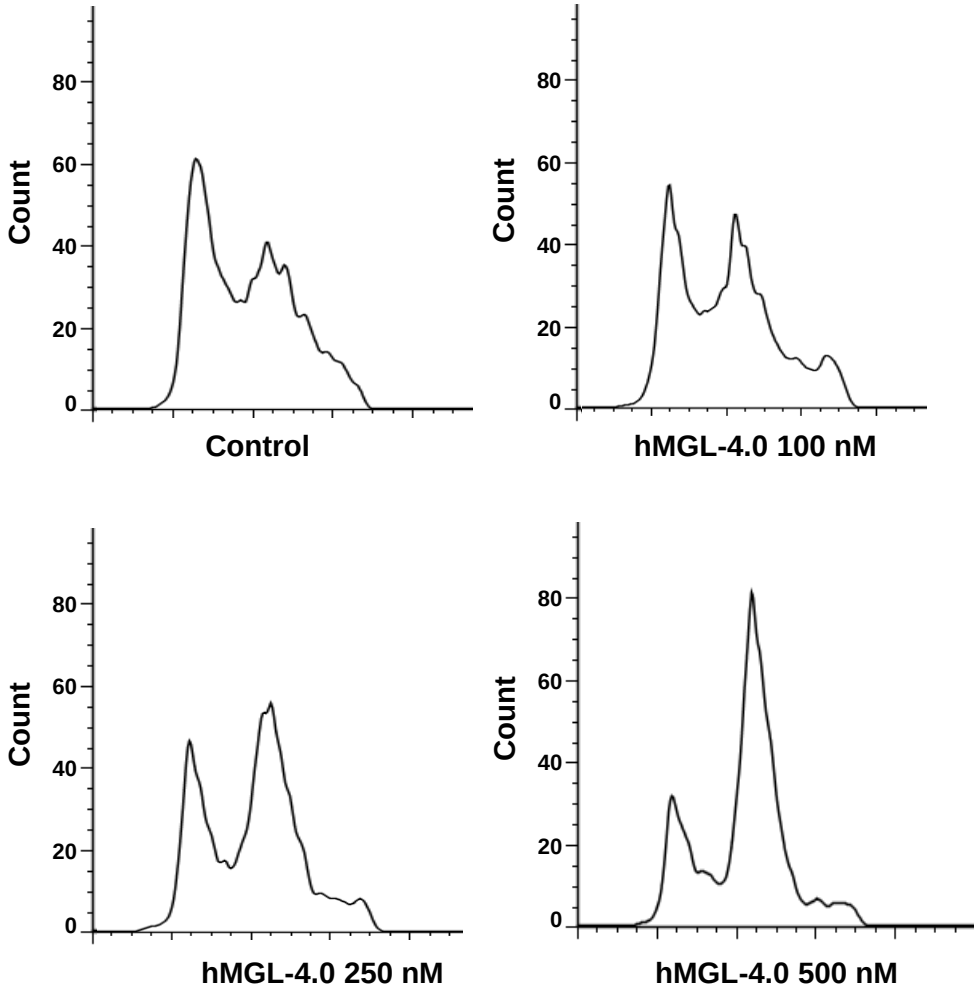

Fig. S9. Effect of hMGL-4.0 treatment in cell cycle distribution.
HMVP2 cells were treated with indicated concentrations of hMGL-4.0 for 24h and Cell-cycle phase distribution was measured by guava based flow cytometry.

Figure S10

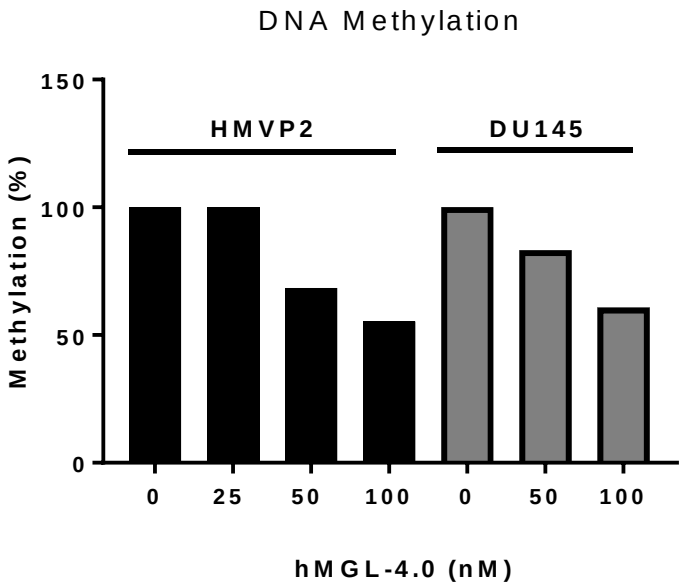

Fig. S10. Effect of hMGL-4.0 on DNA methylation in PCa cells. HMVP2 and DU145 PCa cells were treated with indicated concentrations of hMGL-4.0 for 24 h and global DNA methylation status was measured colorimetrically by ELISA-like format with a commercially available DNA methylation kit (EPIGENTEK). n = 2 cell culture replicates.

Figure S11

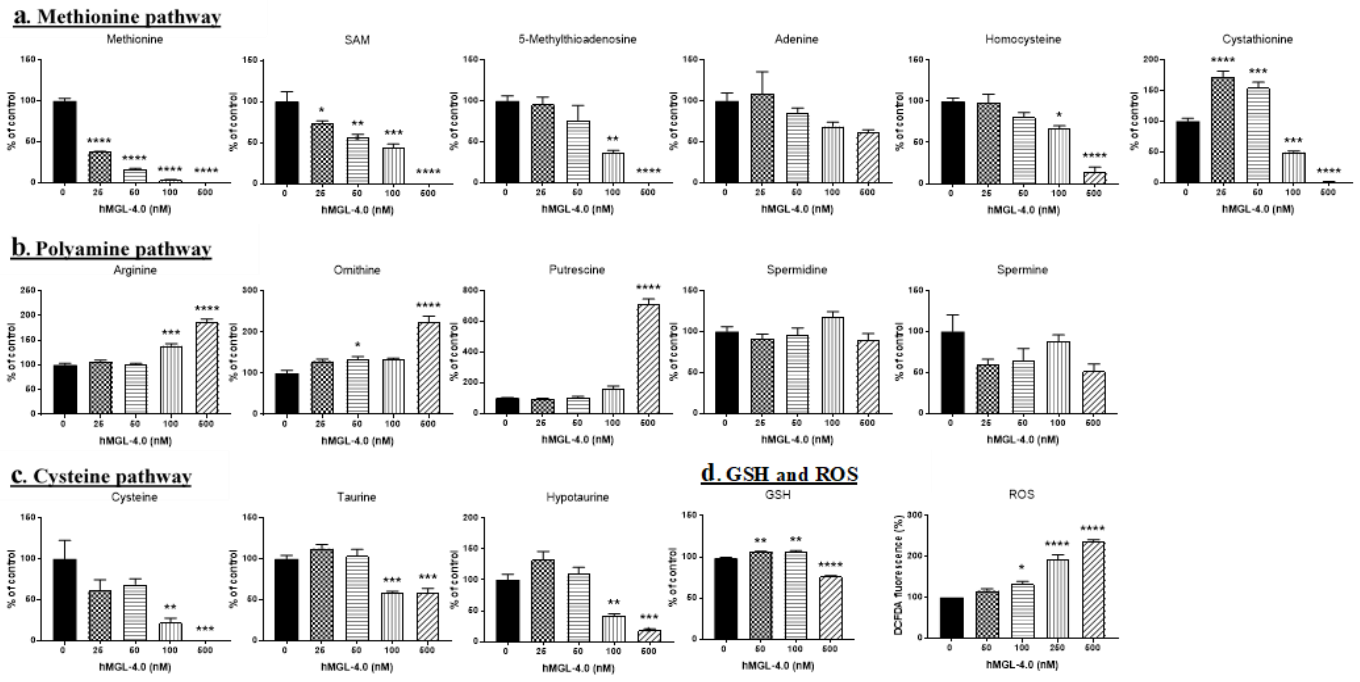

Fig. S11. Metabolomic analyses of 22Rv1 PCa cells following treatment with hMGL-4.0.
(a-d) Relative concentrations of methionine and non-methionine intracellular metabolites in 22Rv1 PCa cells as a function of increasing concentrations of hMGL-4.0 after 24 h treatment as determined by mass spectrometry (n = 3). Measured metabolites in: **(a)** methionine pathway, **(b)** polyamine pathway, **(c)** cysteine pathway, and **(d)** Relative concentrations of GSH and ROS in 22Rv1 PCa cells as a function of increasing concentration hMGL-4.0. GSH level was measured at the 24 h time point by spectrophotometric method (n=3 cell culture replicates at each dose); Cellular ROS levels were measured by 2′,7′-Dichlorofluorescin diacetate (DCFDA) fluorescence 4 h post-treatment (data are from 3 independent experiments). All data are expressed as mean ± s.e.m. One-way ANOVA followed by Bonferroni's multiple comparison test was used for statistical analyses. *P < 0.05; **P < 0.01; *** P < 0.001; **** P < 0.0001.

Figure S12

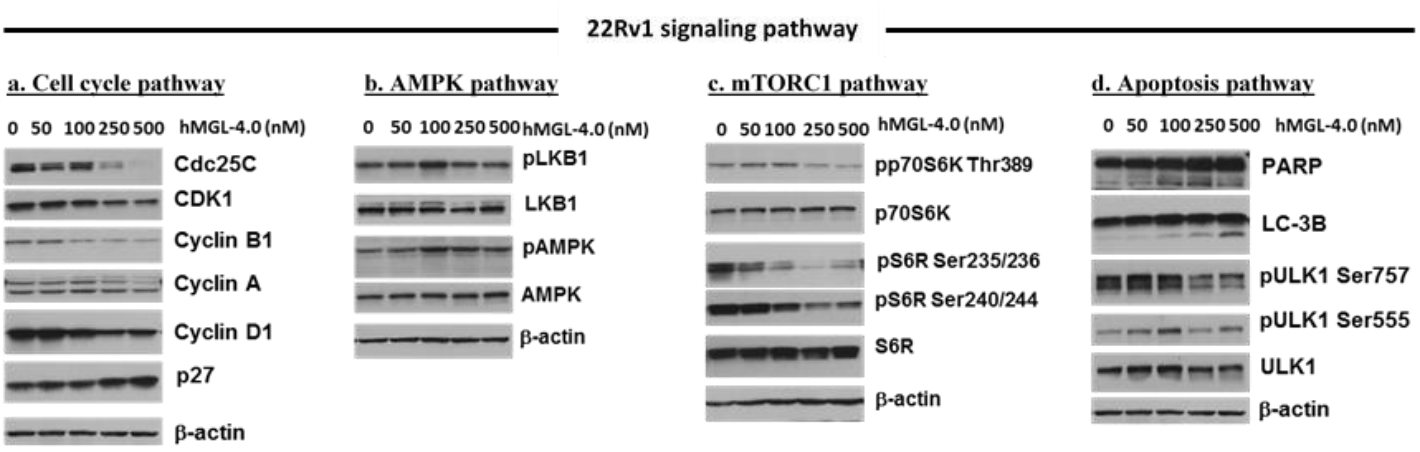

Fig. S12. Signaling pathway analyses of 22Rv1 PCa cells treated with hMGL-4.0. (a-d) 22Rv1 PCa cells were treated with indicated concentrations of hMGL-4.0 for 24 h. Metabolic stress markers and cell cycle regulatory proteins were measured by immunoblot. Immunoblots were performed at least three times with β-actin controls for each experiment.

Figure S13

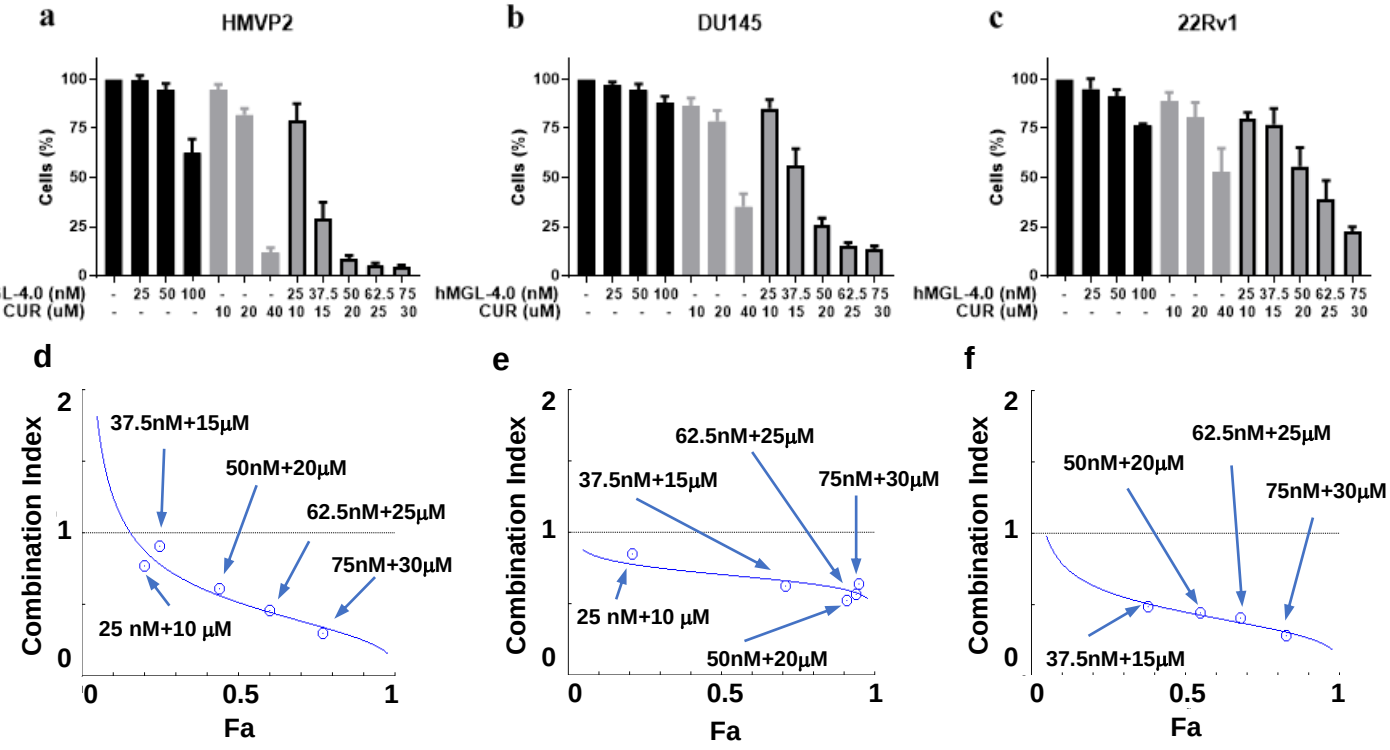

Fig. S13. Synergistic effects of hMGL-4.0 with Curcumin.
(**a-c**) Cell survival as assessed by crystal violet assay following treatment for 72 hours with indicated concentrations of hMGL-4.0, curcumin, or their combination. (**d-f**) combination index plot showing synergistic effects of combinations analyzed by Compusyn software for drug combinations from Combosyn, Inc. Arrows show the combinations of concentrations of Curcumin and hMGL-4.0 (First and second numbers indicate concentrations of hMGL-4.0 and curcumin, respectively)

Figure S14

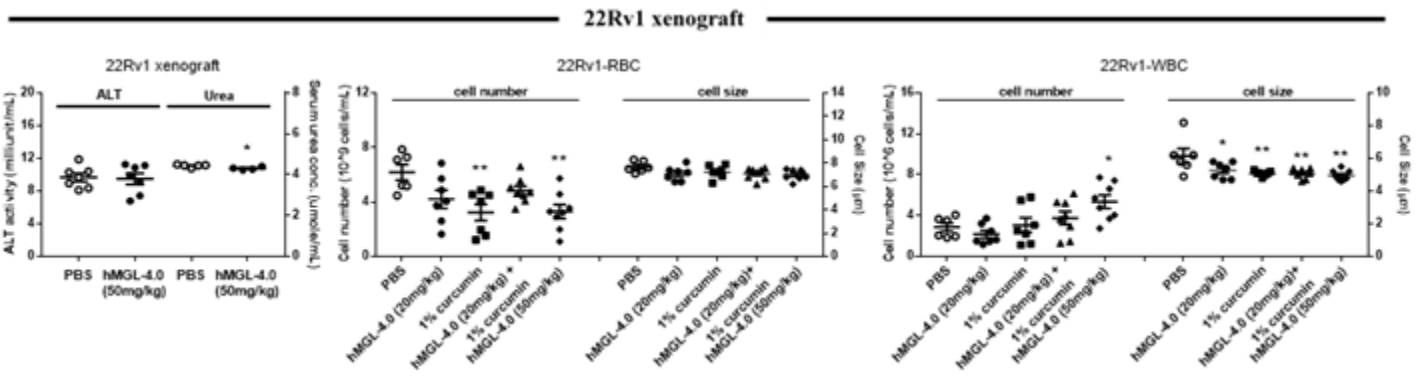

Fig S14. Fig. S5. Toxicological assessment of mice bearing 22Rv1 tumors.
(a) Renal function was assessed by monitoring serum urea concentrations, and liver toxicity was assessed by serum alanine transaminase (ALT) activity following termination of the 22Rv1 xenograft studies (ALT group, n = 7; urea group, n= 5 for control and n=4 for hMGL-4.0 or curcumin or combination treated groups). **(b, c)** Effect of hMGL-4.0 treatment on blood cell count and size, following termination of the 22Rv1 combination treatment xenograft studies: **(b)** red blood cell (RBC) number and size; **(c)** white blood cell (WBC) count and and size**.** Data are expressed as mean ± s.e.m.; two-sided Student's t-test (a) and one-way ANOVA followed by Bonferroni's multiple comparison test (b,c) was used for statistical analyses. *P < 0.05; **P < 0.01.

Figure S15

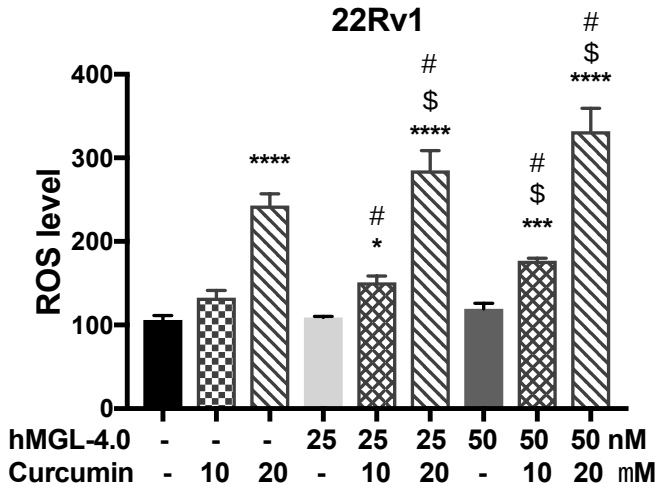

Fig. S15. Synergistic ROS induction of hMGL-4.0 with curcumin.
22Rv1 cells were treated with indicated concentrations of hMGL-4.0, curcumin or their combinations and cellular ROS levels were measured by 2′,7′-Dichlorofluorescin diacetate (DCFDA) fluorescence 24 hr post-treatment. Data are expressed as mean ± s.e.m.; one-way ANOVA followed by Tukey's multiple comparison test. *P < 0.05; ***P < 0.001, ****P < 0.0001 compared to control. $P<0.05 compared to curcumin; #P<0.05 compared to hMGL-4.0.

Figure S16

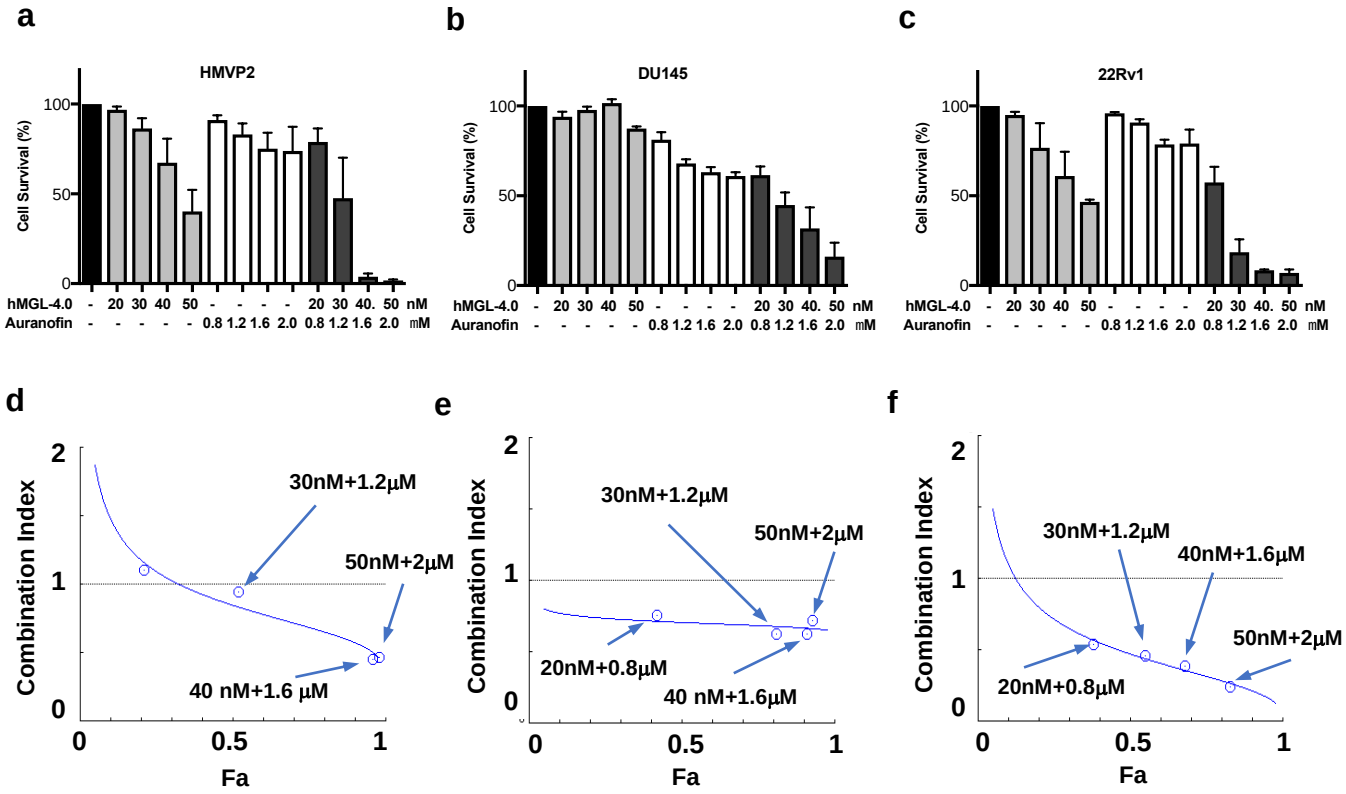

Fig. S16. Synergistic effects of hMGL-4.0 with Auranofin.

(**a-c**) Cell survival as assessed by crystal violet assays following treatment for 72 hr with indicated concentrations of hMGL-4.0, Auranofin, or their combination. (**d-f**) combination index plot showing synergistic effects of combinations analyzed by Compusyn software for drug combinations from Combosyn, Inc. Arrows show the combination of concentrations that produces synergy (First and second number indicates concentrations of hMGL-4.0 and Auranofin, respectively)

Figure S17

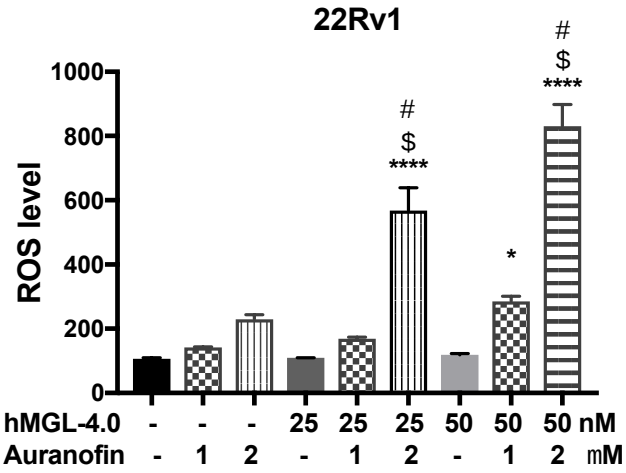

Fig. S17. Synergistic ROS induction of hMGL-4.0 with TXNR inhibitor.
22Rv1 cells were treated with indicated concentrations of hMGL-4.0, auranofin or their combinations and cellular ROS levels were measured by 2′,7′-Dichlorofluorescin diacetate (DCFDA) fluorescence 24 hr post-treatment. Data are expressed as mean ± s.e.m.; one-way ANOVA followed by Tukey's multiple comparison test. *P < 0.05; ****P < 0.0001 compared to control. $P<0.0001 compared to Auranofin; #P<0.0001 compared to hMGL-4.0.